Engineering Solid Mechanics 8 (2020) 187-198

Contents lists available at GrowingScience

Engineering Solid Mechanics

homepage: www.GrowingScience.com/esm

Response of reciprocally supported advanced FRP composite jointed frames - Part 1: Experimental study

Echekwumemchukwu Badifu[a], Alfred Kofi Gand[a*], Messaoud Saidani[a] and Pam Fom[a]

[a]*School of Energy, Construction and Environment, Coventry University, Sir John Laing Building, Coventry, CV1 5FB, United Kingdom*

ARTICLEINFO

Article history:
Received 28 September 2019
Accepted 27 January 2020
Available online
27 January 2020

Keywords:
Pultrusion
GFRP
Reciprocal frames
Mutually supported elements
Ductility
Failure modes

ABSTRACT

This paper reports on a new experimental study for the behaviour of reciprocally connected and supported Fibre Reinforced Polymer (FRP) hollow square profiles axially loaded under several boundary conditions. The study aims to determine the ultimate load of the assembly and failure mechanism of mutually connected units. For the tests, FRP reciprocal frames units (RF) of 100 × 100 × 6.4 mm thick square hollow sections were designed, fabricated and assembled using mechanical fasteners. A bespoke steel test rig allowed for varied support boundary conditions. The observed failure modes were dominated by web buckling, bearing failure around the bolted areas and localised failure. The 100 × 100 mm RF unit achieved the highest load capacity of 16.4 kN and frame stiffness of 1.7 kN/mm, under the pin-pin-roller support boundary conditions. This paper presents the experimental procedure, results and observations.

1. Introduction

Over the years, the use of fibre-reinforced polymer (FRP) for various engineering applications has increased dramatically. The growth in the utilisation of this material has been rapid due to the valuable material properties of FRP. Past laboratory-based research carried on this composite material has led to the implementation of the use of FRP in actual engineering structures. Its applications have been vastly utilised in aerospace and marine technology for over two decades now. In the world of civil engineering, FRP composite is a novel material that has not been vastly used in the wide range of structural engineering applications. Its unique material properties and workability, evident in its application in the marine and aerospace industry gives a glimpse of the immeasurable possibilities of its utilisation in civil and structural engineering. The use of FRP offers an environmentally friendly approach to construction due to its low energy consumption and relatively low carbon emission. Pultrusion is an automated and highly economical process used in the manufacture of uniform cross-sections of FRP. The structural disadvantage of FRP material in comparison with traditional engineering materials, for example, steel, is that FRP has a relatively low modulus of elasticity, low shear strength and its brittle nature (Kara et al. 2013). However, there are potentials to overcome these disadvantages with appropriate structural configuration. This is viable in the sense that the stiffness is improved in a framed structure, as the

* Corresponding author.
E-mail addresses: a.gand@coventry.ac.uk (A. K. Gand)

doi: 10.5267/j.esm.2020.1.005

mechanical performance is dependent on the structural assembly rather than the material itself. This, therefore, increases the potentials for the use of FRP in frame structures, since framed structures are subjected to mainly axial loading (Gand et al. 2013, Jia et al. 2016, Luo et al. 2015). A three-dimensional load distribution path is obtained from a space frame configuration. Therefore, this could introduce some level of deformation before collapse thereby offering substantial ductility to FRP, thus limiting the effects of its brittle nature. However, since the structural members in a space frame are predominantly subjected to axial loading, an adequate design of its compressive members may offer a substantial amount of non-linear deformation (Chilton, 2007). Adequate design of these compression members requires details of the mechanical behaviour of Pultruded Fibre-reinforced polymer (PFRP) reciprocal frames, which seem very limited, as not much research has been carried out in this context.

Applications of FRP in the space frame are quite limited. Bai & Yang (2013) tested square hollow sections of FRP in an all-composite space frame assembly using glass fibre reinforced polymer (GFRP) connectors (Yu & Xiao, 2013). Results showed predominant shear failure around surfaces to the bolted connections. However, this is less likely to be the case in the same assembly with circular GFRP as is expected that there will be minimal contact between the shear connectors and GFRP. Some studies have focused on the workability of adhesive connections in mutually connected FRP (Gonilha et al., 2014; Green & Phillips, 1982; Hagio et al., 2003; Hollaway et al., 1990; Keller & Gürtler 2006; Keller et al., 2007; Kostopoulos et al., 2005; Pickett et al., 1982). Small-scale FRP composite space frame structures were investigated as far back as 1982 where Green and Phillip suggested a crimp-bonded joint for circular FRP pultruded sections bonded with alloy using a structural adhesive paste (Green & Phillips, 1982). Picket et al. (1982) used the same approach to develop a composite of FRP and steel space frame for the construction of a pedestrian bridge. This FRP had inner aluminium linings, which were threaded for connectors screwed at the node joints (Pickett et al., 1982). Holloway et al. (1990) further generated an enhanced joint by filling nylon with glass and sticking to the caps of FRP tubes and designing a composite plate to sandwich both tubes. Stainless steel was used to form a joint for GFRP space frame, utilising diagonal connections between the GFRP in the assembly using bolts and tested experimentally (Hagio et al*.,* 2003). Studies on large-scale space frame structure are even more limited using FRP. A 13,776 kg weight single lane traffic bridge spanning 11.6 m was designed with a space frame where the GFRP hollow sections were connected with steel box element covering the nodal joints (Kostopoulos et al., 2005). A longer span, 12 m hybrid composite emergency bridge consisting of an aluminium deck supported by FRP truss was designed having steel connections to avoid premature shear failure (Zhang et al., 2014). This advancement has been useful. However, the connections required cumbersome and precise processes.

A more simplified and practical approach was established to produce a lightweight modular space frame structure by bonding steel tubes to each end of spherical sectional PFRP tubes using adhesives. The end of the circular steel tubes was flattened to ease connections with other members at the node joints using mechanical bolts/fasteners. Bonding FRP and steel tubes with adhesives mitigate the possibilities of pull out shear failure observed the by researchers when holes for the bolts are drilled in PFRP (Yang et al., 2016; Yang et al., 2015b). Adhesive bonding has been noted to be capable of transferring uniform load with less stress concentration when compared with bold joints (Keller & Vallée 2005). Another hybrid with about the connection configuration as Keller et al*.,* 2005 was designed. The bridge, which weighs 773 kg and spans 8m, is 1.6 m wide and 1.13 m deep was supported by a space frame structure consisting circular hollow section FRP, bonded with steel tubes at both ends, with the steel having a flat end for easy assembly at the nodal joints (Yang et al., 2015a). For application as a pedestrian bridge, the overall stiffness and load-carrying capacity were satisfactory. Hizam et al. (2019) evaluated the behaviour of pultruded FRP truss system with mechanically inserted through-bolts. In the study, composite trusses were fabricated using pultruded FRP closed sections. At the truss joints, a mechanical steel closed section was inserted into the FRP tubes locally and secured with adhesive bond. This then facilitated the individual truss elements to be joined via through-bolts. By adopting approach at the joints, the local bearing stress concentrations across the thickness of the joint components were

streamlined resulting in increased load carrying capacity of the joints, and consequently the capacity of the truss system.

This paper presents an experimental study of the interaction mode at the joints of connected pultruded FRP as a reciprocal frame (RF) under varying support boundary conditions. Presented in Fig. 1 is the schematic disposition of the frame. Reciprocal frame arrangement made of steel members has been the subject of previous research (Rizzuto et al., 2000; Rizzuto et al., 2001; Rizzuto & Popovic, 2010). Furthermore, the mechanical behaviour of the bolted connections, load transfer pattern of the RF unit, deformation orientation, failure mode, displacement and energy absorbing capacity of the entire PFRP jointed system under axial load is considered.

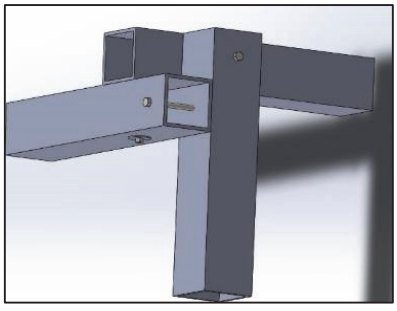

Fig. 1. Schematics of RF assembly

2. Methodology

In this section, the materials used for the reciprocally supported FRP joints systems, assembly of samples and test protocols are discussed.

2.1 Materials, specimen preparation and assembly

2.1.1 Pultruded FRP profiles

FRP box sections of nominal size 100 × 100 × 6.4 mm was used to develop all RF units. The profiles were supplied courtesy of Engineered Composites Ltd, UK. Each profile was machine cut to the nominal length, approximately, 505 mm.

Table 1. Material properties assumed for test profiles (EUROCOMP, 1996)

Property	Units	Longitudinal	Transverse
Tensile Strength	N/mm^2	410	44
Tensile Modulus	kN/mm^2	27	3.5
Compressive Strength	N/mm^2	270	-
Compressive Modulus	kN/mm^2	24	4.5
Shear Strength (in-plane)	N/mm^2	15	-
Shear Modulus (in-plane)	kN/mm^2	4.2	-
Flexural Strength	N/mm^2	400	115
Flexural modulus	kN/mm^2	14	8
Poisson's Ratio		0.2	0.1

The machined edges of the profiles were further smoothened and trimmed to a length of 504 mm using abrasive sandpaper to ensure an even end of the beams for uniform load distribution. In the absence of full material characterisation and testing on full profiles and coupons, the FRP profiles assume the minimum range of mechanical properties presented in Table 1. The properties outlined apply to box profiles with web thickness greater than 6 mm. Pultruded FRP properties are reproduced from the EUROCOMP Design Code and Handbook (Clarke, 1996), and conform to the minimum values for grade E23 in the European Standard EN 13706-3:2002 (2002), which define the material specifications for pultruded FRPs.

2.1.2 Connecting dowels, nuts and washers

Stainless steel dowel, 10 mm in diameter, with associated nuts and washer were used in the joint configuration and assembly. The bolt system was preloaded to a bolt torque for the snug-fit condition. The bolt setting out satisfy the minimum requirements recommended for geometric parameters (Bank, 2006), as presented in Table 2. To achieve a uniform distribution of load, all elements were assembled with a 100 mm clearance at the top creating a hollow opened square section at the apex to allow for a 100 mm solid square load node. Each element is mutually supporting each other at the approximately 200 mm from the top of each profile while the remaining 300 mm of each profile extends to the steel plates of the test rig presented in Fig. 2. Each profile mutually supported together at the bolts points such that each profile is laid in a perpendicular position to the other. The opposite ends, first edges of the profiles had the bolts located at 50 mm from the top of the profiles while the second opposite ends of the profiles had the bolt located at 150 mm from the top end.

Table 2. Recommended Geometric relations for lap joint connections (Bank, 2006)

	Research parameters		Manufacturer	
	Recommended	Minimum	Recommended	Minimum
End distance to bolt diameter (e_1/d)	≥3	2	≥3	2
Width to bolt diameter (w/d)	≥5	3	≥4	3
Side distance to bolt diameter (e_2/d)	≥2	1.5	≥2	1.5
Pitch distance to bolt diameter (p/d)	≥4	3	≥5	4
Gauge distance to bolt diameter (g/d)	≥4	3	≥5	4
Bolt dimeter to thickness (d/t)	≥1	0.5	≥2	1
Washer diameter to bolt diameter (d_w/d)	≥2	2	-	-
Bolt-hole clearance (d_n-d)	Tight-fit (0.05d)	1.6 (Max.)	1.6	-

2.2 Experimental test programme

To evaluate the mechanical behaviour, strength and stability, three reciprocally supported FRP joint system were tested under various support boundary conditions. This section details the optimisation of boundary conditions and the experimental programme.

2.2.1 Test rig

Presented in Fig. 2 is a bespoke steel frame support rig incorporating end plates oriented at 45 degrees at all three support ends to restrain any movement of the elements of the RF unit. To facilitate lateral movement, 4 mm diameter ball bearings were placed under each cut arm of the rig.

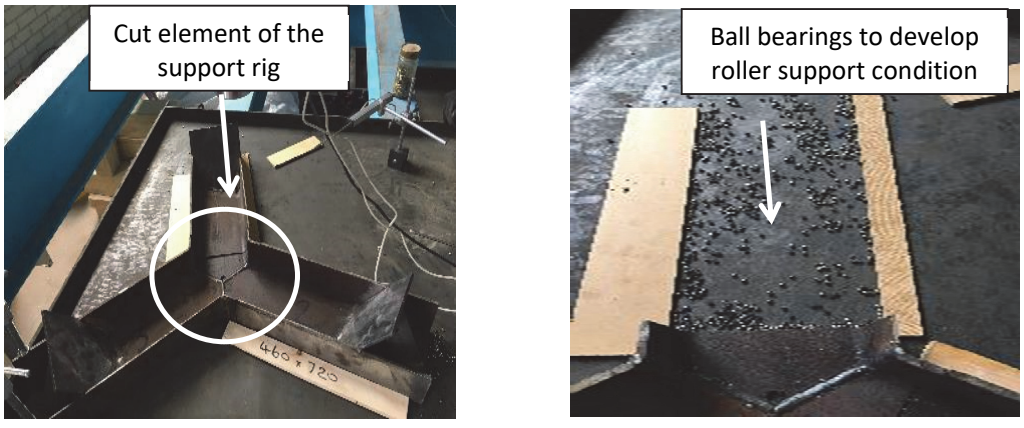

Fig. 2. Frame support arrangement

2.2.2 Test set-up and instrumentations

Presented in Fig. 3 are components and arrangements of the specimen preparation and assembly. Each element of the specimen was labelled; thus, E1, E2 and E3. The elements were assembled with 10

mm diameter stainless steel dowels, nuts and washers. One arm of the designed support rig was cut to create a free boundary condition. Steel ball bearings were placed underneath the cut arm of the support to allow for lateral movement, thus simulating a roller support condition. While the other two arms of the support rig clamped to the steel base of the test rig to prevent movement of the respective arms (that is two elements pinned and one unrestrained in the lateral direction). Subsequently, two cut bases supported on ball bearing was placed underneath the bases while one base remained clamped. The clamped bases mimicked pinned support condition, with the bases on ball bearings allowing mimicking roller support boundary condition. In the final test series, ball bearings were placed underneath all isolated bases, i.e. roller support condition. Table 3 presents the support description. Post yield strain gauges (TML type PFL-30-11) was secured on each engaging element on two opposing faces. The strain gauges were located 250 mm from the top edge of each engaging element. The location of the strain gauges was determined to avoid the interactive influence of adjoining FRP elements. After carefully placing RF units in the test rig, the load was applied using a manually operated hydraulic pump, under load control. To record the applied load, a 100 kN rated load cell was adopted. Each RF unit was loaded until failure. The load, global vertical and lateral displacement (from LVDTs, DT1 to DT5) and strain data were recorded at 0.1 s intervals using the Geodatlog 8 control system. After each test, the RF unit was inspected for observed failure modes and damage. Presented in Figs. 4 and 5 are the schematic and actual test arrangements, respectively. Fig. 6 shows the strain gauge locations.

(a) RF assembly modules

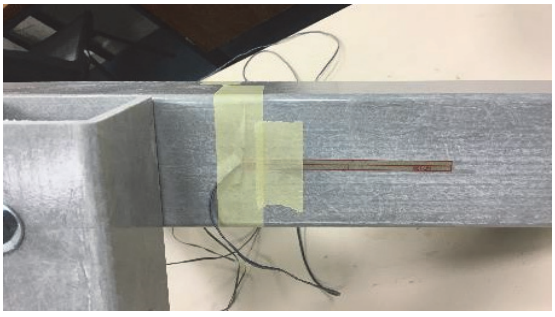

(b) Typical strain gauge location

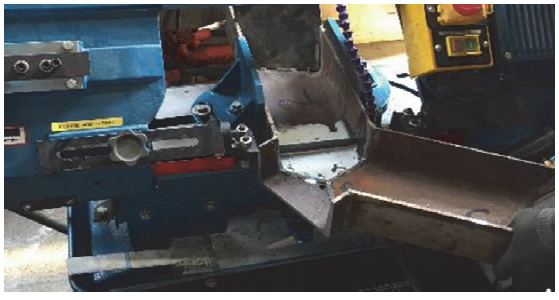

(c) Modification of support rig

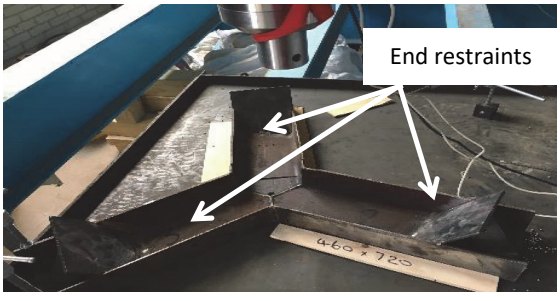

(d) Base support configuration

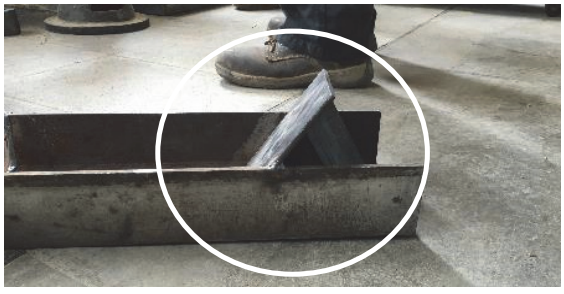

(e) End restraints, typical

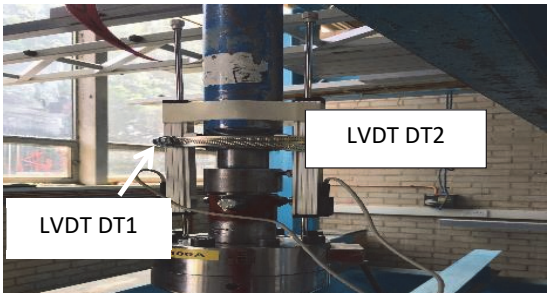

(f) Displacement transducers

Fig. 3. (a) – (f) specimen, test rig schematic and test system

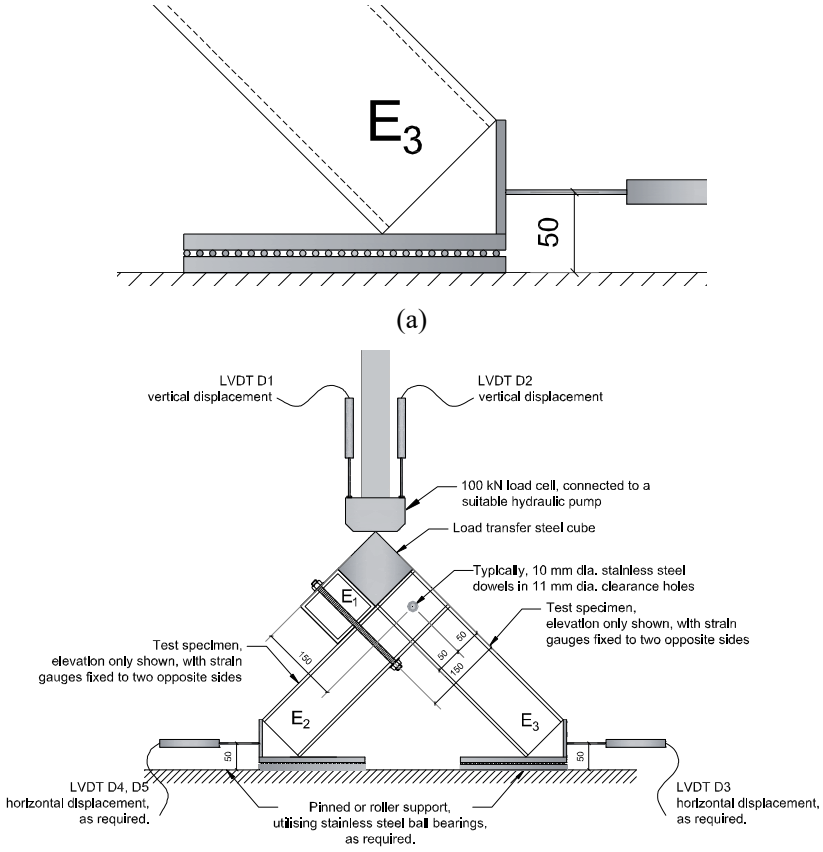

Fig. 4. (a) Schematic test arrangements, (b) close up view of ball bearing type 'roller' support

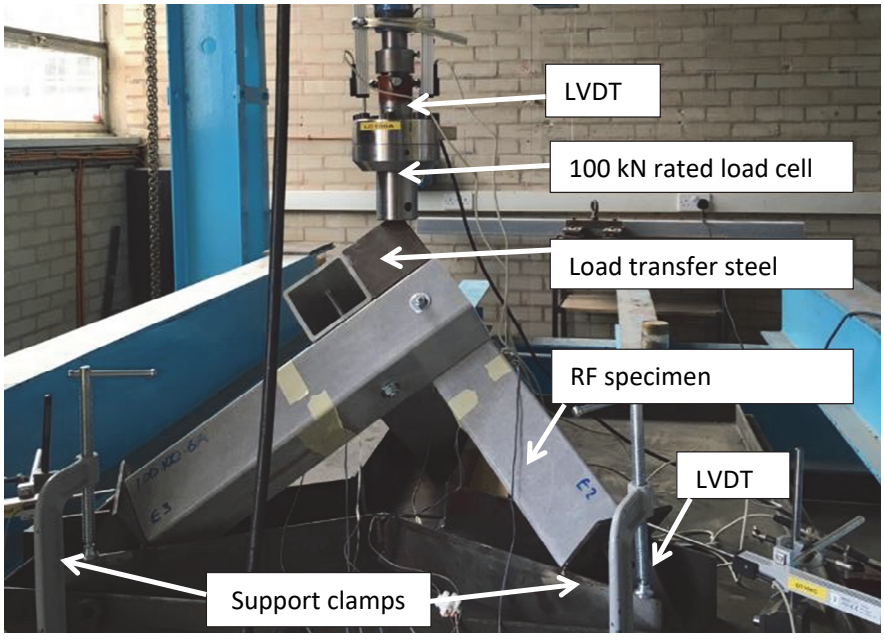

Fig. 5. Experimental test set-up

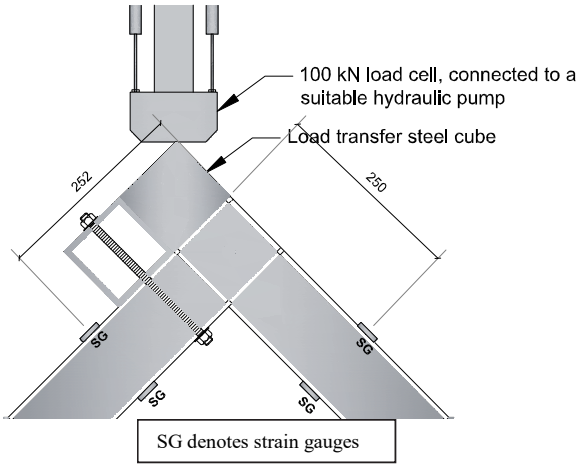

Fig. 6. Locations of strain gauges.

Table 3. Specimen and support condition details

Specimen ID	Support reference	Support definition
100-6a-SP1	SP1	Pin-pin-roller
100-6b-SP2	SP2	Pin-roller-roller
100-6c-SP3	SP3	Roller-roller-roller

3. Results and discussion

3.1 Failure mechanism of RF units

Pultruded FRP lapped joints are associated with four principal failure modes – bearing, net-tension, shear-out, and cleavage failures. These are illustrated in Fig. 7. These modes of failure were expected in the RF joint assembly tested. Three principal failure modes were observed – localised bearing failure, web buckling, and longitudinal cracks and laminate splitting, as detailed in Fig. 8.

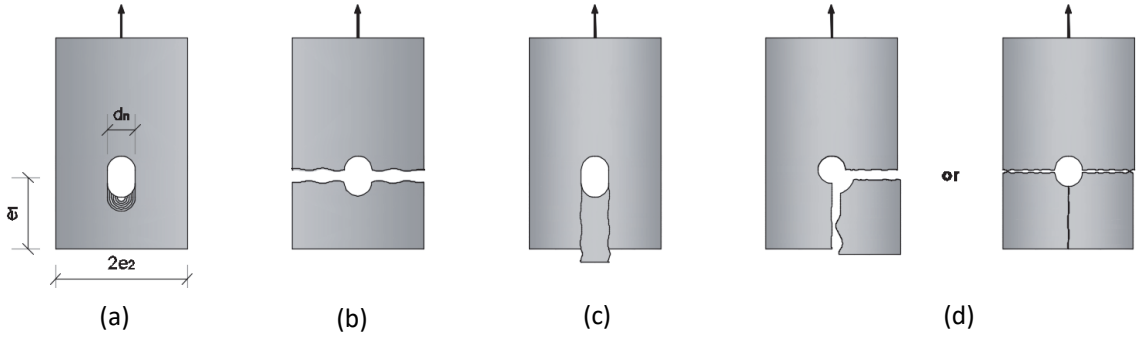

Fig. 7. Plate-to-plate distinct modes of failure with a single steel bolt: (a) bearing; (b) net-tension; (c) shear-out; (d) cleavage (based on Mottram, 2011).

3.1.1 Failure mechanism for specimen 100-6a-SP1

Specimen 100-6a-SP1 exhibited significant bearing failure at the contact point between the mechanical fastener and FRP, which initiated web buckling on the FRP. While failure at the same point on the opposite end of the FRP element (E1) was the development of crack propagation which was as a result of the failure of the web

to accommodate the stresses induced by the mechanical fastener. The presence of the penny washer eliminated a bearing failure at the tensile zone (E1 Bottom). Cracks developed on all four corners of the pinned elements (E1 & E2) of the RF assembly, owing to the thickness and minimal corner radius of the FRP sections while the roller element (E3) experienced fewer cracks and bearing failure, as illustrated in Fig. 8.

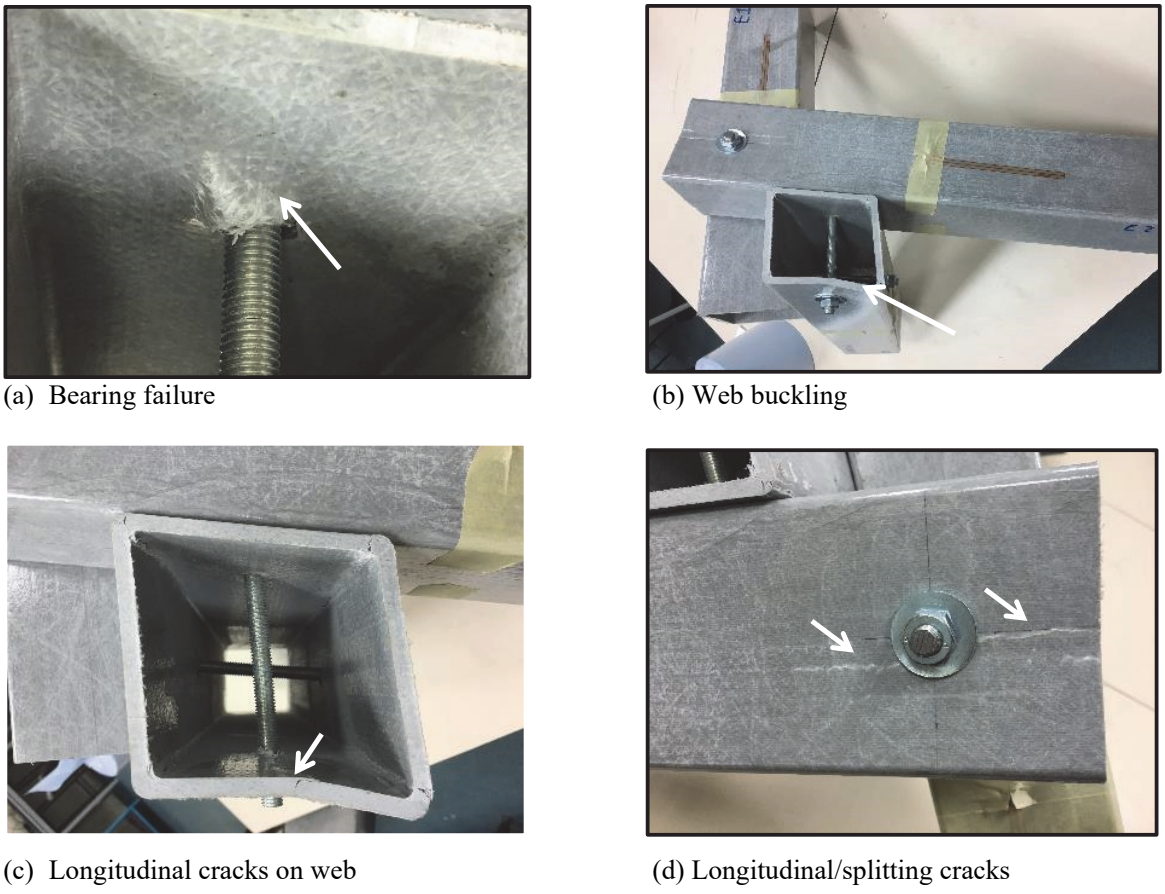

(a) Bearing failure (b) Web buckling

(c) Longitudinal cracks on web (d) Longitudinal/splitting cracks

Fig. 8. Failure mechanism of 100-6a-SP1

3.1.2 Failure mechanism for specimen 100-6b-SP2

Specimen 100-6b-SP2 exhibited similar failure modes as 100-6a-SP1. Bearing failure was significant on the pinned element E1 with lamina tearing and crack propagation on all four corners similar to E1 & E2 in SP1 configuration. While E2 & E3 exhibited minimal shear failure by the area of contact with mechanical fasteners. Little slip away from original alignment at the joint areas was noticed on E2 and E3. The modes of failure are shown in Fig. 9.

3.1.3 Failure mechanism for specimen 100-6c-SP3

The specimen exhibited localised failure at the apex of the RF unit where the load node was placed. Disorientation at the joint including large slips from the original alignment of the assembly. This was primarily due to the large displacement at all elements in the assembly. Bearing failure by the axis of mechanical fasteners and minimal cracks, however not as much observed with all other RF assembly, as shown in Fig. 10.

(a) Web-flange junction fracture/tearing

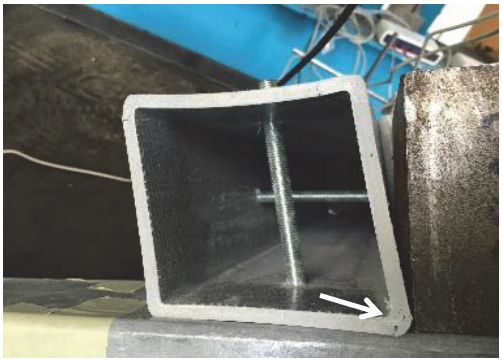

(b) Crack propagation

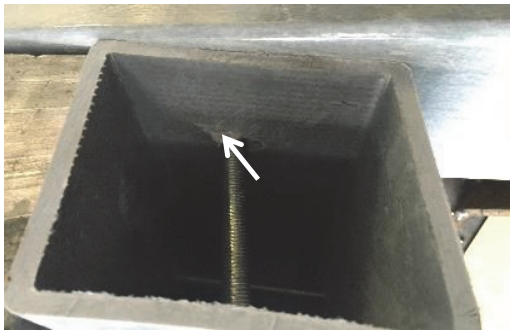

(c) Bearing failure

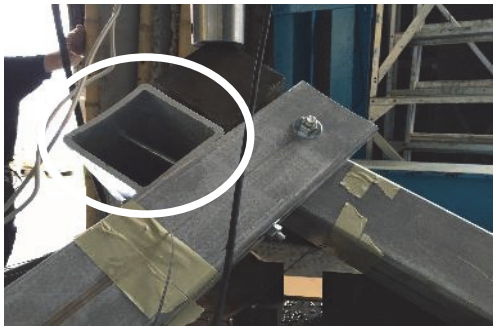

(d) Deformed profile

Fig. 9. Failure mechanism of specimen 100-6b-SP2.

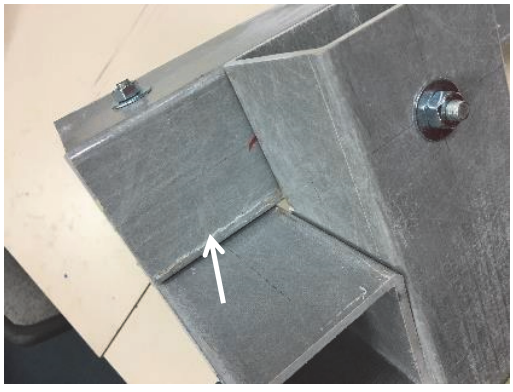

(a) Localised failure at load node interface

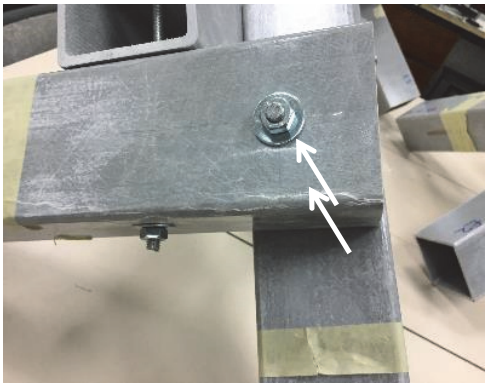

(b) Localised failure are profile edge

(c) Separated interface between elements

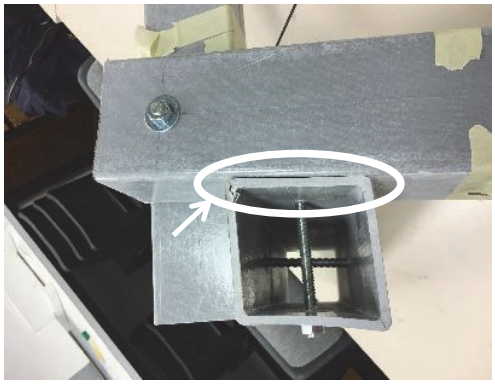

(d) Slip at element interface

Fig. 10. Failure mechanism of specimen 100-6c-SP3.

3.2 Load-displacement response

Presented in Fig. 11 are the load-displacement responses of the three specimens tested. Each assembly displayed a linear load-displacement relationship up to 70% of their respective ultimate load. The frame incorporating pin-pin-roller support condition, i.e. specimen SP1 achieved the highest load capacity of 16.4 kN, to be followed by specimen SP2 and SP3, with ultimate loads of 15.8 kN and 15.1 kN, respectively. There is a marginal difference between the ultimate loads for all RF configuration unlike their respective displacements of 16.7 mm, 23.5 mm and 32.1 mm. Initially, all the frames displayed a linear elastic behaviour. The behaviour of the specimens was observed up to the ultimate load to evaluate the stiffness and ductility of the frame assembly. Results show that specimen 100 × 100 - 6a under the SP1 support condition was stiffer than the counterpart frames. The stiffness corresponds with the minimal displacement detailed in Table 4.

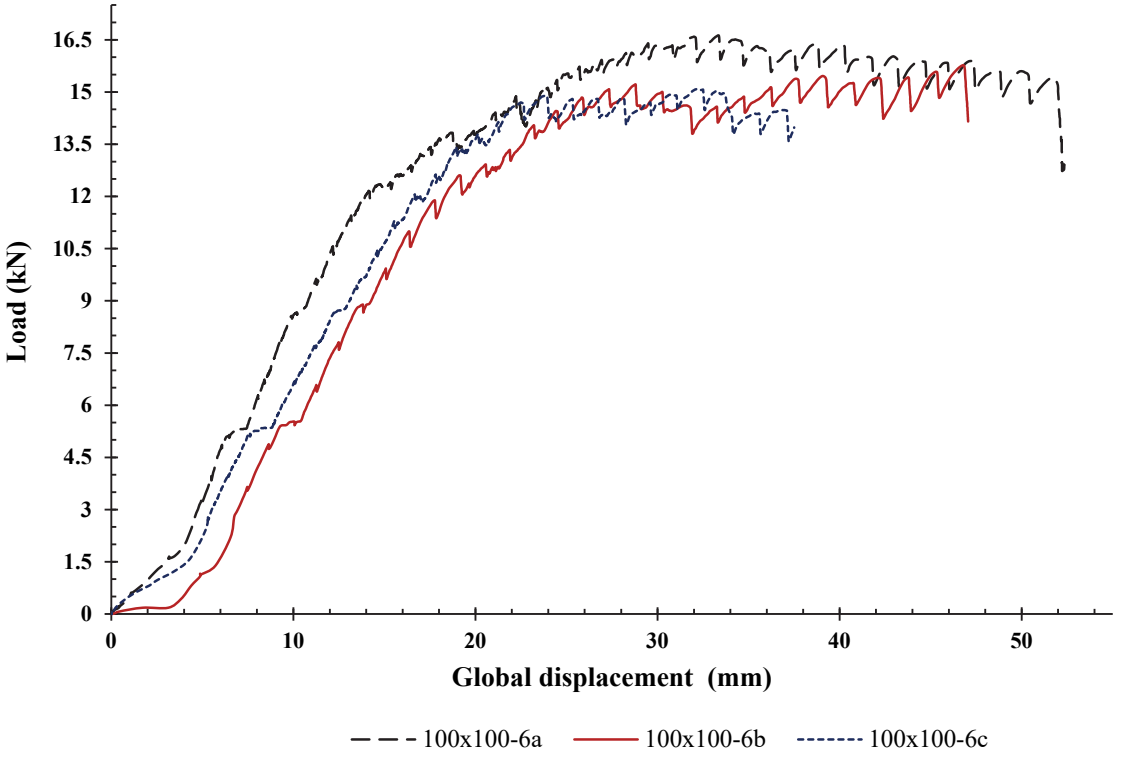

Fig. 11. Load-displacement plots for all specimens

Table 4. Summary of results of all test specimens

Specimen ID	Boundary condition	Frame stiffness, K	Maximum load, P_{ult}	Global displacement at maximum load δ_{ult}	Yield load, P_y	Displacement at yield δ_y	δ_{ult}/δ_y
		kN/mm	kN	mm	kN		
100-6a-SP1	SP1	1.72	16.4	16.7	12.2	7.7	2.18
100-6b-SP2	SP2	1.52	15.8	23.5	11.6	9.1	2.58
100-6c-SP3	SP3	0.79	15.1	32.1	11.6	16.1	1.99
	Mean	1.34	15.78	24.1	11.8	11.0	2.25
	SD	0.34	0.53	6.30	0.28	3.67	0.25

where SD is the standard deviation, and δ_{ult}/δ_y = ductility index

4. Concluding remarks

The experimental study in this paper provided a further understanding of the behaviour of new reciprocally and mutually connected pultruded FRP joint systems. The frame units are capable of being adaptable to create large-scale space truss structure. Three specimens were fabricated and tested under the same joint configuration under three different boundary conditions. The end conditions had a minimal effect on the load-carrying capacity of the RF unit with a maximum of up 7.9% difference. However, a significant effect of the end conditions was observed in the frame stiffness with a 44% difference between pin-pin-roller support and roller-roller-roller support condition. As was expected, the absence of end restrictions on the roller-roller-roller support condition resulted in a global displacement of 32.1 mm, twice as much as the displacement recorded for pin-pin-roller support condition and 26% more than that of pin-roller-roller support condition. Based on the test data, observations and the ensuing analyses, the following concluding remarks are made:

1. The load-displacement responses of the frame unit show initial linear elastic behaviour. However, the load distribution path for the frame was not uniform for all assembly.
2. The pin-pin-roller support boundary condition achieved the highest load carrying capacity and frame stiffness.
3. The first point of failure is the contact area between the mechanical fastener and FRP. The magnitude of disorientation at the joint is dependent on the global stiffness.
4. The expected failure mode for RF with this assembly is predominantly bearing failure in the areas of tensile stress concentration.
5. The support boundary condition type directly influences the frame stiffness.

Acknowledgement

The authors are particularly thankful to the technicians at the School of Energy, Construction and Environment, Coventry University, for their assistance in the fabrication of the test specimens. The authors also gratefully acknowledge the support of Engineered Composites, UK, and supplier of the pultruded FRP box profiles.

References

Bank, L. C. (2006). Composites for Construction: Structural Design with FRP Material. John Wiley & Sons, Inc., Hoboken, New Jersey, USA.

BS EN 13706-3. (2002). Reinforced plastics composites. Specifications for pultruded profiles. - Part 3: Specific requirements, British Standards Institution.

Chilton, J. (2007). *Space Grid Structures*: Routledge.

Clarke, J.L. (Ed.). (1996). Structural design of polymer composites - EUROCOMP Design Code and Handbook, E. & F.N. Spon, London.

Gand, A. K., Chan, T., & Mottram, J. T. (2013). Civil and Structural Engineering Applications, Recent Trends, Research and Developments on Pultruded Fiber Reinforced Polymer Closed Sections: A Review. *Frontiers of Structural and Civil Engineering,* 7(3), 227-244.

Gonilha, J. A., Barros, J., Correia, J. R., Sena-Cruz, J., Branco, F. A., Ramos, L. F., Gonçalves, D., Alvim, M. R., & Santos, T. (2014). Static, Dynamic and Creep Behaviour of a Full-Scale GFRP-SFRSCC Hybrid Footbridge. *Composite Structures* 118(1), 496-509.

Green, A. K., & Phillips, L. N. (1982). Crimp-Bonded End Fittings for use on Pultruded Composite Sections. *Composite Structures.* 13(3), 219-224.

Hagio, H., Utsumi, Y., Kimura, K., Takahashi, K., Itohiya, G., & Tazawa, H. (2003). Development of space truss structure using glass fibre reinforced plastics. Proceedings: Advanced Materials for Construction of Bridges, Buildings, and Other Structures III, Davos, Switzerland, 7–12 September. ECI Digital Archives

Hizam, R. M., Manalo, A. C., Karunasena, W. & Bai, Y. (2019). Behaviour of pultruded GFRP truss system connected using through-bolt with mechanical insert. *Composites Part B - Engineering*, 168, 44-57.

Hollaway, L., Romhi, A., & Gunn, M. (1990). Optimisation of Adhesive Bonded Composite Tubular Sections. *Composite Structures,* 16(1-3), 125-170.

Jia, L. F., Yu, B., Xiao, Y., & Ye, L. (2016). Bolted Sleeve Joints for Connecting Pultruded FRP Tubular Components. *Journal of Composites for Construction,* 20(1), 04015024.

Kara, I. F., Ashour, A. F., & Dundar, C. (2013). Deflection of Concrete Structures Reinforced with FRP Bars. *Composites Part B - Engineering,* 44, 375-84.

Keller, T., Schaumann, E., & Vallée, T. (2007). Flexural Behaviour of a Hybrid FRP and Lightweight Concrete Sandwich Bridge Deck'. *Composites Part A: Applied Science and Manufacturing,* 38(3), 879-889.

Keller, T., & Gürtler, H. (2006). Design of Hybrid Bridge Girders with Adhesively Bonded and Compositely Acting FRP Deck. *Composite Structures*, 74(2), 202-212.

Keller, T., & Vallée, T. (2005). Adhesively Bonded Lap Joints from Pultruded GFRP Profiles. Part I: Stress-Strain Analysis and Failure Modes. *Composites Part B: Engineering,* 36(4), 331-340.

Kostopoulos, V., Markopoulos, Y. P., Vlachos, D. E., Katerelos, D., Galiotis, C., Tsiknias, T., Zacharopoulos, D., Karalekas, D., Chronis, P., & Kalomallos, D. (2005). Design and Construction of a Vehicular Bridge made of glass/polyester Pultruded Box Beams. *Plastics, Rubber and Composites,* 34(4), 201-207.

Luo, F. J., Bai, Y., Yang, X., & Lu, Y. (2015). Bolted Sleeve Joints for Connecting Pultruded FRP Tubular Components. *Journal of Composites for Construction,* 20(1), 04015024.

Mottram, J. T., & Zafari, B. (2011). Pin-bearing Strengths for Design of Bolted Connections in Pultruded Structures. *Structures and Buildings,* 164(5), 291-305.

Pickett, A., Hollaway, L., & Phillips, L. N. (1982). Analysis of a Crimped and Bonded Joint for Load Bearing Skeletal Members. *Composite Structures,* 13(3), 257-267.

Rizzuto, J.P, Saidani, M., & Chilton, J. C. (2000). The Self-supporting multi-reciprocal Grid (MRG) system using notched elements, *Journal of the International Association for Shell and Spatial Structures*, 41(2), 125–131.

Rizzuto, J.P, Saidani, M., & Chilton, J. C. (2001). Polyhedric space structures using reciprocally supported elements of various cross-section", *Journal of the International Association for Shell and Spatial Structures*, 42(3), 149–159.

Rizzuto, J. P., & Popovic, L. O. (2010). Connection Systems in Reciprocal Frames and Mutually supported elements. Space Structure Networks. *International Journal of Space Structures,* 25(4), 243-256.

Yang, X., Bai, Y., Luo, F. J., Zhao, X., & He, X. (2016). Fiber-Reinforced Polymer Composite Members with Adhesive Bonded Sleeve Joints for Space Frame Structures. *Journal of Materials in Civil Engineering,* 29(2), 04016208.

Yang, X., Bai, Y., & Ding, F. (2015a). Structural Performance of a Large-Scale Space Frame Assembled using Pultruded GFRP Composites. *Composite Structures,* 133, 986-996.

Yang, X., Bai, Y.. & Ding, F. (2015b). Structural Performance of a Large-Scale Space Frame Assembled using Pultruded GFRP. *Composite Structures,* 133, 986-96.

Yu, B., & Xiao, Y. (2013). Novel Joint for Assembly of all-composite Space Truss Structures: Conceptual Design and Preliminary Study. *Journal of Composites for Construction,* 17(1), 130-138.

Zhang, D., Zhao, Q., Huang, Y., Li, F., Chen, H.. & Miao, D. (2014). Flexural Properties of a Lightweight Hybrid FRP-Aluminum Modular Space Truss Bridge System. *Composite Structures,* 108(1), 600-615.